

## VISCOUS DISSIPATION EFFECTS IN A VERTICAL ANNULUS FILLED WITH FLUID-SATURATED POROUS MEDIUM

Eduard Marušić-Paloka and Igor Pažanin

**ABSTRACT.** The investigation of heat transfer within porous medium has attracted considerable interest because of its growing practical importance. The present paper is devoted to the study of a steady-state non-isothermal fluid flow through a vertical cylindrical annulus filled with sparsely packed porous medium. The governing system is given by the Darcy-Brinkman-Boussinesq model where the heat equation includes the viscous dissipation term. The side walls are maintained at uniform temperatures, while the flow is driven by the axial pressure gradient. Introducing the thickness of the annular region as the small parameter of the problem, the goal is to derive the approximation of the flow via asymptotic analysis. Although the governing problem is coupled and nonlinear, the asymptotic solution is proposed in the explicit form and that represents our main contribution. As such, it clearly displays the effects of porous structure and viscous dissipation on the temperature and velocity distribution. Due to the viscous dissipation, we observe the increase in the heat generation leading to a raise in the temperature and velocity profile within the annulus. Moreover, it is deduced that reducing the thickness of the annular region may be employed to strengthen the seepage velocity of the working fluid.

### 1. Introduction

As a local production of thermal energy induced by viscous forces in fluid-particle interactions, the viscous dissipation effect is an important phenomenon that cannot be neglected in porous medium flows. If we compare it with other thermal effects relevant to fluid flow (for instance, with the thermal buoyancy coming from the heated or cooled walls), it turns out that the consequent mechanical energy can have a serious impact on the effective behavior of the fluid flow (see e.g. [1]). A significant viscous dissipation naturally occurs in numerous practical applications. The examples range from geological processes (petroleum reserves, geothermal reservoirs, etc.) to industrial applications (catalytic reactors, porous

---

2020 *Mathematics Subject Classification*: 35B40, 35Q35, 76S05.

*Key words and phrases*: cylindrical annulus, viscous dissipation, porous medium, asymptotic analysis.

journal bearings, etc.). In view of that, the current problem acknowledging this phenomenon has been extensively studied in the literature. For the overview of the obtained results, we refer to the chapter [2].

If one wants to study a non-isothermal, creeping fluid flow within a sparsely packed porous medium, the Brinkman-extended Darcy system is the right choice (see e.g. [3–5]) coupled with the energy equation via Boussinesq approximation. Thus, in a steady-state regime, the seepage velocity  $\mathbf{u}^* = (u_1^*, u_2^*, u_3^*)$ , the pressure  $p^*$  and the temperature  $T^*$  of the fluid obey the following system (see e.g. [6]):

$$(1.1) \quad \frac{\mu}{k} \mathbf{u}^* - \mu_{eff} \Delta \mathbf{u}^* + \nabla p^* = \rho_f [1 - \alpha(T^* - T_r)] \mathbf{g},$$

$$(1.2) \quad \operatorname{div} \mathbf{u}^* = 0,$$

$$(1.3) \quad -\lambda \Delta T^* + \rho_f C_f \mathbf{u}^* \cdot \nabla T^* = \Phi^*.$$

Let us address the given positive constants in (1.1)–(1.3). The parameters of the porous medium are the permeability  $k$  and the thermal conductivity  $\lambda$ . The saturating fluid is characterized by the density  $\rho_f$ , the physical viscosity  $\mu$  and the effective viscosity of the Brinkman term  $\mu_{eff}$ . Its thermal characteristics are given by the specific heat (at constant volume)  $C_f$  and the coefficient of thermal expansion  $\alpha$ . The reference temperature of the surrounding medium is  $T_r$ , whereas the gravitational force is denoted by  $\mathbf{g}$ .

In the above system, the viscous dissipation effect appears as an extra term  $\Phi^*$  on the right-hand side in the temperature equation. This term may take various forms depending on the way how we model the momentum equations. When the Brinkman second-order term in (1.1) is present, the following form of the viscous dissipation function is widely accepted:

$$(1.4) \quad \Phi^* = \frac{\mu}{k} [(u_1^*)^2 + (u_2^*)^2 + (u_3^*)^2] + \mu_{eff} \left[ 2 \left( \frac{\partial u_1^*}{\partial x_1^*} \right)^2 + 2 \left( \frac{\partial u_2^*}{\partial x_2^*} \right)^2 + 2 \left( \frac{\partial u_3^*}{\partial x_3^*} \right)^2 \right] \\ + \mu_{eff} \left[ \left( \frac{\partial u_1^*}{\partial x_2^*} + \frac{\partial u_2^*}{\partial x_1^*} \right)^2 + \left( \frac{\partial u_1^*}{\partial x_3^*} + \frac{\partial u_3^*}{\partial x_1^*} \right)^2 + \left( \frac{\partial u_2^*}{\partial x_3^*} + \frac{\partial u_3^*}{\partial x_2^*} \right)^2 \right].$$

The formula (1.4) was originally proposed by Al-Hadhrami et al. [7]. It keeps the dissipation  $\Phi^*$  always positive and, most importantly, ensures the asymptotic behavior remaining correct for a wide range of permeability values  $k$ . It is composed of two parts: the first one results from the internal heating needed to extrude the fluid through the porous medium (the first term-Darcy dissipation) and the second part results from the the frictional heating due to dissipation (the remaining two terms).

Due to its practical importance, heat transfer processes in an annular region have been the subject of numerous studies. We point out to the study [8], providing a nice overview of the experimental and numerical studies on thermal flows through a vertical annulus. In particular, the porous medium flows through vertical annular regions have been the subject of many research efforts (see e.g. [9, 10] for the experimental results and e.g. [11–13] for numerical simulations). The objective here is to analytically study the fluid flow through a porous medium in a vertical annulus by focusing on the thermal effects due to the viscous dissipation.

We consider the system (1.1)–(1.4) in the domain  $\Omega^*$  defined as the region between two vertical concentric cylinders of different radii ( $R_1 < R_2$ ) (see Figure 1). The co-ordinate system  $Ox_1^*x_2^*x_3^*$  is posed such that  $\mathbf{g} = -g\mathbf{e}_3$  ( $g > 0$ ). The domain  $\Omega^*$  is assumed to be either thin or long by taking  $\frac{R_2 - R_1}{R_1} \ll 1$ . A fluid-saturated sparsely packed porous medium is filling the domain  $\Omega^*$  whose side walls are kept at uniform temperatures. The axial pressure gradient governs the porous medium flow through the annulus. Such setting naturally arises in the above-mentioned applications and, thus, has attracted attention in the last two decades (see e.g. [14–16]).

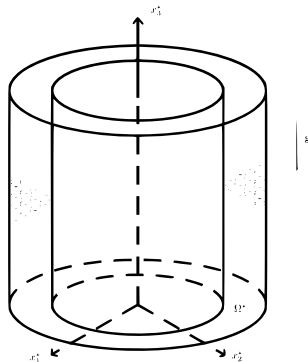


FIGURE 1. The domain  $\Omega^*$  defined as the region between two vertical concentric cylinders of radii  $R_1 < R_2$  and filled with a porous medium of permeability  $k$  and thermal conductivity  $\lambda$ .

Let us provide more bibliographic remarks related to the subject of the paper. The analytical studies of the viscous dissipation effects in porous media flow are not so frequent throughout the literature. Indeed, the analysis of simple 2D channel flows are mostly available with only Darcy dissipation appearing in (1.4) ( $k \rightarrow 0$ ), see e.g. [17–21]. Starting from the decoupled problem, a rigorous derivation of a higher-order model for a 3D thin domain involving viscous dissipation effects as in (1.4) has been presented in [22]. A simplified version of (1.4) has been considered in [23] to investigate a heat and fluid flow through a vertical annulus via homotopy perturbation method. In view of that, here we aim to analytically tackle the fully coupled problem (1.1)–(1.4) in a vertical annulus. To accomplish that, we extend the approach from [24, 25] employed for a thin porous domain without the presence of the viscous dissipation.

We compose the paper as follows. Section 2 is devoted to the formal setting of the problem and its transformation to dimensionless form. Passing to the cylindrical coordinates, in Section 3, the approximation of the solution is proposed, using the asymptotic expansion in powers of the small parameter  $\varepsilon = \frac{R_2 - R_1}{R_1}$ . After computing the zero-order approximation of the flow (Section 3.1), we construct the correctors in the asymptotic expansion for the fluid velocity and temperature (Section 3.2). By doing that, we capture the effects of all physically relevant phenomena

occurring in the system and increase the accuracy of the approximation. We point out that the asymptotic solution has been computed in the explicit form enabling us to clearly visualize the impact of the viscous dissipation term on the effective flow (Section 4). In Section 5, we summarize the obtained results and indicate the future research directions based on this paper.

## 2. Formulation of the problem

As described above, the considered domain reads as follows:

$$(2.1) \quad \Omega^* = \{\mathbf{x}^* = (x_1^*, x_2^*, x_3^*) \in \mathbf{R}^3 : R_1^2 < (x_1^*)^2 + (x_2^*)^2 < R_2^2, 0 < x_3^* < \ell\}.$$

The cylindrical annulus  $\Omega^*$  is assumed to be filled by a porous medium described by the Darcy-Brinkman-Boussinesq equations. Taking into account the viscous dissipation, we arrive at the following system:

$$(2.2) \quad \frac{\mu}{k} \mathbf{u}^* - \mu_{eff} \Delta \mathbf{u}^* + \nabla p^* = \rho_f [1 - \alpha(T^* - T_r)] \mathbf{g} \quad \text{in } \Omega^*,$$

$$\operatorname{div} \mathbf{u}^* = 0 \quad \text{in } \Omega^*,$$

$$(2.3) \quad -\lambda \Delta T^* + \rho_f C_f \mathbf{u}^* \cdot \nabla T^* = \Phi^* \quad \text{in } \Omega^*,$$

where

$$\begin{aligned} \Phi^* = & \frac{\mu}{k} \left[ (u_1^*)^2 + (u_2^*)^2 + (u_3^*)^2 \right] + \mu_{eff} \left[ 2 \left( \frac{\partial u_1^*}{\partial x_1^*} \right)^2 + 2 \left( \frac{\partial u_2^*}{\partial x_2^*} \right)^2 + 2 \left( \frac{\partial u_3^*}{\partial x_3^*} \right)^2 \right] \\ & + \mu_{eff} \left[ \left( \frac{\partial u_1^*}{\partial x_2^*} + \frac{\partial u_2^*}{\partial x_1^*} \right)^2 + \left( \frac{\partial u_1^*}{\partial x_3^*} + \frac{\partial u_3^*}{\partial x_1^*} \right)^2 + \left( \frac{\partial u_2^*}{\partial x_3^*} + \frac{\partial u_3^*}{\partial x_2^*} \right)^2 \right]. \end{aligned}$$

We impose the no-slip boundary condition on the side walls of the annular region which are maintained at constant temperatures  $T_1, T_2$  ( $T_1 > T_2$ ):

$$(2.4) \quad \mathbf{u}^* = 0 \quad \text{for } |\tilde{\mathbf{x}}^*| = \sqrt{(x_1^*)^2 + (x_2^*)^2} = R_i, \quad i = 1, 2,$$

$$(2.5) \quad T^* = T_i \quad \text{for } |\tilde{\mathbf{x}}^*| = R_i, \quad i = 1, 2.$$

We refer the reader to [2, 6] with regard to governing equations and the boundary conditions. To analyze the impact of the porous structure and viscous dissipation, it is feasible to write the governing problem in dimensionless form. We proceed as follows (see e.g. [26]):

$$\begin{aligned} \mathbf{x} &= \frac{\mathbf{x}^*}{R_1}, \quad \mathbf{u}^\varepsilon = \rho_f C_f R_1 \frac{\mathbf{u}^*}{\lambda}, \quad T^\varepsilon = \frac{T^* - T_2}{T_1 - T_2}, \\ p^\varepsilon &= \frac{\rho_f C_f k}{\mu \lambda} [p^* + \rho_f g (1 + \alpha(T_r - T_2)) x_3^*], \\ \gamma &= \frac{\mu_{eff}}{\mu}, \quad Da = \frac{k}{R_1^2} \quad (\text{Darcy number}), \\ Ra &= \frac{\rho_f^2 C_f (R_2 - R_1)}{\mu \lambda} k g \alpha (T_1 - T_2) \quad (\text{Rayleigh-Darcy number}), \\ Br &= \frac{\mu U_0^2}{\lambda (T_1 - T_2)} \quad (\text{Brinkman number}), \end{aligned}$$

where  $U_0 = \frac{\lambda}{\rho_f C_f R_1}$  is chosen as the reference velocity and  $\varepsilon = \frac{R_2 - R_1}{R_1}$  is the small parameter of the problem. As a result, the equations (2.2)–(2.3) become:

$$(2.6) \quad \mathbf{u}^\varepsilon - \gamma Da \Delta \mathbf{u}^\varepsilon + \nabla p^\varepsilon = \frac{1}{\varepsilon} Ra T^\varepsilon \mathbf{e}_3 \quad \text{in } \Omega^\varepsilon,$$

$$(2.7) \quad \operatorname{div} \mathbf{u}^\varepsilon = 0 \quad \text{in } \Omega^\varepsilon,$$

$$(2.8) \quad -\Delta T^\varepsilon + \mathbf{u}^\varepsilon \cdot \nabla T^\varepsilon = Br \left\{ \frac{1}{Da} \left[ (u_1^\varepsilon)^2 + (u_2^\varepsilon)^2 + (u_3^\varepsilon)^2 \right] \right. \\ \left. + \gamma \left[ 2 \left( \frac{\partial u_1^\varepsilon}{\partial x_1} \right)^2 + 2 \left( \frac{\partial u_2^\varepsilon}{\partial x_2} \right)^2 + 2 \left( \frac{\partial u_3^\varepsilon}{\partial x_3} \right)^2 \right] \right. \\ \left. + \gamma \left[ \left( \frac{\partial u_1^\varepsilon}{\partial x_2} + \frac{\partial u_2^\varepsilon}{\partial x_1} \right)^2 + \left( \frac{\partial u_1^\varepsilon}{\partial x_3} + \frac{\partial u_3^\varepsilon}{\partial x_1} \right)^2 + \left( \frac{\partial u_2^\varepsilon}{\partial x_3} + \frac{\partial u_3^\varepsilon}{\partial x_2} \right)^2 \right] \right\} \quad \text{in } \Omega^\varepsilon,$$

where

$$\Omega^\varepsilon = \left\{ \mathbf{x} = (x_1, x_2, x_3) \in \mathbf{R}^3 : 1 < x_1^2 + x_2^2 < (1 + \varepsilon)^2, 0 < x_3 < \frac{\ell}{R_1} \right\}.$$

Note that the boundary conditions (2.4)–(2.5) transform into:

$$(2.9) \quad \mathbf{u}^\varepsilon = 0 \quad \text{for } |\tilde{\mathbf{x}}| = \sqrt{x_1^2 + x_2^2} = 1, \quad |\tilde{\mathbf{x}}| = 1 + \varepsilon,$$

$$(2.10) \quad T^\varepsilon = 1 \quad \text{for } |\tilde{\mathbf{x}}| = 1,$$

$$(2.11) \quad T^\varepsilon = 0 \quad \text{for } |\tilde{\mathbf{x}}| = 1 + \varepsilon.$$

It should be observed that the governing problem is nonlinear and coupled, so our goal is to build the approximate solution of the system (2.6)–(2.11). Due to the geometry of the domain, it is natural to assume that the flow is axisymmetric and this is the only additional assumption related to the current problem.

### 3. Analysis

In order to construct the approximation of the solution  $(\mathbf{u}^\varepsilon, p^\varepsilon, T^\varepsilon)$ , we use the approach from [24, 25] (see also [27]). The methodology is based on the multiscale asymptotic expansion technique with respect to the annulus thickness  $\varepsilon$ , representing the small parameter of the problem. The goal is to compute the higher-order terms in the expansion in order to construct more accurate asymptotic approximation.

Taking into account the domain (2.1), the natural step is to pass to cylindrical coordinates. However, before that, we notice that

$$\nabla \mathbf{u}^\varepsilon + (\nabla \mathbf{u}^\varepsilon)^T = \begin{bmatrix} 2 \frac{\partial u_1^\varepsilon}{\partial x_1} & \frac{\partial u_1^\varepsilon}{\partial x_2} + \frac{\partial u_2^\varepsilon}{\partial x_1} & \frac{\partial u_1^\varepsilon}{\partial x_3} + \frac{\partial u_3^\varepsilon}{\partial x_1} \\ \frac{\partial u_2^\varepsilon}{\partial x_1} + \frac{\partial u_1^\varepsilon}{\partial x_2} & 2 \frac{\partial u_2^\varepsilon}{\partial x_2} & \frac{\partial u_2^\varepsilon}{\partial x_3} + \frac{\partial u_3^\varepsilon}{\partial x_2} \\ \frac{\partial u_3^\varepsilon}{\partial x_1} + \frac{\partial u_1^\varepsilon}{\partial x_3} & \frac{\partial u_3^\varepsilon}{\partial x_2} + \frac{\partial u_2^\varepsilon}{\partial x_3} & 2 \frac{\partial u_3^\varepsilon}{\partial x_3} \end{bmatrix}$$

so that the heat equation (2.8) can be compactly rewritten as

$$(3.1) \quad -\Delta T^\varepsilon + \mathbf{u}^\varepsilon \cdot \nabla T^\varepsilon = Br \left( \frac{1}{Da} |\mathbf{u}^\varepsilon|^2 + \frac{\gamma}{2} |\nabla \mathbf{u}^\varepsilon + (\nabla \mathbf{u}^\varepsilon)^T|^2 \right).$$

The flow is assumed to be axisymmetric so we introduce

$$r = \sqrt{x_1^2 + x_2^2}, \quad z = x_3$$

and use the known expressions for the differential operators in cylindrical coordinates (see e.g. [28]). For  $\mathbf{u}^\varepsilon = u_r^\varepsilon \mathbf{e}_r + u_z^\varepsilon \mathbf{e}_3$ , the equations (2.6)–(2.7) and (3.1) become:

$$(3.2) \quad \begin{aligned} u_r^\varepsilon - \gamma Da \left( \frac{\partial^2 u_r^\varepsilon}{\partial r^2} + \frac{1}{r} \frac{\partial u_r^\varepsilon}{\partial r} - \frac{u_r^\varepsilon}{r^2} + \frac{\partial^2 u_r^\varepsilon}{\partial z^2} \right) + \frac{\partial p^\varepsilon}{\partial r} &= 0, \\ u_z^\varepsilon - \gamma Da \left( \frac{\partial^2 u_z^\varepsilon}{\partial r^2} + \frac{1}{r} \frac{\partial u_z^\varepsilon}{\partial r} + \frac{\partial^2 u_z^\varepsilon}{\partial z^2} \right) + \frac{\partial p^\varepsilon}{\partial z} &= \frac{1}{\varepsilon} Ra T^\varepsilon, \\ \frac{\partial u_r^\varepsilon}{\partial r} + \frac{u_r^\varepsilon}{r} + \frac{\partial u_z^\varepsilon}{\partial z} &= 0, \end{aligned}$$

$$(3.3) \quad - \left( \frac{\partial^2 T^\varepsilon}{\partial r^2} + \frac{1}{r} \frac{\partial T^\varepsilon}{\partial r} + \frac{\partial^2 T^\varepsilon}{\partial z^2} \right) + u_r^\varepsilon \frac{\partial T^\varepsilon}{\partial r} + u_z^\varepsilon \frac{\partial T^\varepsilon}{\partial z} = Br \left\{ \frac{1}{Da} \left[ (u_r^\varepsilon)^2 + (u_z^\varepsilon)^2 \right] \right. \\ \left. + \gamma \left[ 2 \left( \frac{\partial u_r^\varepsilon}{\partial r} \right)^2 + 2 \left( \frac{\partial u_z^\varepsilon}{\partial z} \right)^2 + \frac{2}{r^2} (u_r^\varepsilon)^2 + \left( \frac{\partial u_r^\varepsilon}{\partial z} + \frac{\partial u_z^\varepsilon}{\partial r} \right)^2 \right] \right\},$$

for  $r \in \langle 1, 1 + \varepsilon \rangle$ ,  $z \in \langle 0, \frac{\ell}{R_1} \rangle$ . Now, expanding the unknown functions in powers  $\varepsilon$

$$(3.4) \quad \mathbf{u}^\varepsilon(r, z) = \mathbf{u}^0 \left( \frac{r-1}{\varepsilon}, z \right) + \varepsilon \mathbf{u}^1 \left( \frac{r-1}{\varepsilon}, z \right) + \dots,$$

$$p^\varepsilon(r, z) = \frac{1}{\varepsilon^2} p^0 \left( \frac{r-1}{\varepsilon}, z \right) + \frac{1}{\varepsilon} p^1 \left( \frac{r-1}{\varepsilon}, z \right) + \dots,$$

$$(3.5) \quad T^\varepsilon(r, z) = T^0 \left( \frac{r-1}{\varepsilon}, z \right) + \varepsilon T^1 \left( \frac{r-1}{\varepsilon}, z \right) + \dots$$

we plug it to the system (3.2)–(3.3). By looking at the terms with equal powers of  $\varepsilon$ , we deduce the recursive sequence of boundary-value problems and solve it simultaneously by acknowledging the imposed conditions (2.9)–(2.11).

**3.1. The approximation at the main order.** Introducing the dilated variable

$$\xi = \frac{r-1}{\varepsilon},$$

we first obtain:

$$(3.6) \quad \frac{1}{\varepsilon^3} : \frac{\partial p^0}{\partial \xi} = 0 \Rightarrow p^0 = p^0(z),$$

$$(3.7) \quad \frac{1}{\varepsilon^2} : -\gamma Da \frac{\partial^2 u_r^0}{\partial \xi^2} + \frac{\partial p^1}{\partial \xi} = 0,$$

$$(3.8) \quad \frac{1}{\varepsilon^2} : -\gamma Da \frac{\partial^2 u_z^0}{\partial \xi^2} + \frac{dp^0}{dz} = 0,$$

$$(3.9) \quad \frac{1}{\varepsilon} : \frac{\partial u_r^0}{\partial \xi} = 0 \Rightarrow u_r^0 = u_r^0(z),$$

$$(3.10) \quad \frac{1}{\varepsilon^2} : -\frac{\partial^2 T^0}{\partial \xi^2} = \gamma Br \left( \frac{\partial u_z^0}{\partial \xi} \right)^2.$$

Hereinafter, on the left hand side of the equations we indicate the order of the equations with respect to the small parameter  $\varepsilon$ .

Since  $u_r^0(0, z) = u_r^0(1, z) = 0$ , from (3.6) and (3.8) we obtain

$$u_r^0 = 0, \quad p^1 = p^1(z).$$

Solving (3.7), we obtain

$$(3.10) \quad u_z^0(\xi, z) = \frac{1}{2Da} \xi(\xi - 1) \frac{dp^0}{dz},$$

due to the fact that  $u_z^0(0, z) = u_z^0(1, z) = 0$ . Applying (3.10) to (3.9) leads to

$$-\frac{\partial^2 T^0}{\partial \xi^2} = \frac{Br}{\gamma Da^2} \left( \xi^2 - \xi + \frac{1}{4} \right) \left( \frac{dp^0}{dz} \right)^2.$$

Taking into account that  $T^0(0, z) = 1$  and  $T^0(1, z) = 0$  (see (2.10)–(2.11)), after integrating with respect to  $\xi$ , we obtain

$$(3.11) \quad T^0(\xi, z) = \frac{Br}{2\gamma Da^2} \left( \frac{\xi^3}{3} - \frac{\xi^4}{6} - \frac{\xi^2}{4} + \frac{\xi}{12} \right) \left( \frac{dp^0}{dz} \right)^2 + (1 - \xi).$$

To complete the derivation of the zero-order approximation, the pressure  $p^0$  still needs to be determined. From the  $\mathcal{O}(1)$ -term in the divergence equation we have

$$(3.12) \quad 1 : \frac{\partial u_r^1}{\partial \xi} + \frac{\partial u_z^0}{\partial z} = 0.$$

Since  $u_r^1(0, z) = u_r^1(1, z) = 0$ , a simple integration with respect to  $\xi$  yields

$$(3.13) \quad \frac{dp^0}{dz} = C = \text{const.}$$

which is exactly the axial pressure gradient given in advance.

**3.2. Correctors.** To obtain a more accurate approximation, we continue and build the correctors  $(u^1, p^1, T^1)$  in the asymptotic expansions (3.4)–(3.5). The next-order terms are given by the following equations:

$$(3.14) \quad \frac{1}{\varepsilon} : -\gamma Da \frac{\partial^2 u_r^1}{\partial \xi^2} + \frac{\partial p^2}{\partial \xi} = 0,$$

$$(3.15) \quad \frac{1}{\varepsilon} : -\gamma Da \left( \frac{\partial^2 u_z^1}{\partial \xi^2} + \frac{\partial u_z^0}{\partial \xi} \right) + \frac{dp^1}{dz} = RaT^0,$$

$$(3.16) \quad \varepsilon : \frac{\partial u_r^2}{\partial \xi} + \xi \frac{\partial u_r^1}{\partial \xi} + u_r^1 + \frac{\partial u_z^1}{\partial z} + \xi \frac{\partial u_z^0}{\partial z} = 0,$$

$$(3.17) \quad \frac{1}{\varepsilon} : -\frac{\partial^2 T^1}{\partial \xi^2} + \frac{\partial T^0}{\partial \xi} = 0.$$

Before tackling the above system, we go back to (3.12) and deduce that  $\frac{\partial u_r^1}{\partial \xi} = 0$ , due to (3.10) and (3.13). In view of that, from (3.14) we conclude

$$u_r^1 = 0, \quad p^2 = p^2(z).$$

Now, we solve the equation (3.15) by applying the derived expressions for  $u_z^0$  and  $T^0$  (see (3.10) and (3.11)). We arrive at

$$(3.18) \quad u_z^1(\xi, z) = -\frac{1}{2\gamma Da} \left( \frac{\xi^3}{3} - \frac{\xi^2}{2} + \frac{\xi}{6} \right) \frac{dp^0}{dz} + \frac{1}{2\gamma Da} (\xi^2 - \xi) \frac{dp^1}{dz} \\ + \frac{RaBr}{2\gamma^2 Da^3} \left( \frac{\xi^6}{180} - \frac{\xi^5}{60} + \frac{\xi^4}{48} - \frac{\xi^3}{72} + \frac{\xi}{240} \right) \left( \frac{dp^0}{dz} \right)^2 \\ - \frac{Ra}{\gamma Da} \left( \frac{\xi^3}{6} - \frac{\xi^2}{4} + \frac{\xi}{12} \right).$$

Note that we took into account that  $u_z^1(0, z) = u_z^1(1, z) = 0$ . Having in mind that  $u_r^1 = 0$ ,  $\frac{\partial u_z^0}{\partial z} = 0$ ,  $u_r^2(0, z) = u_r^2(1, z) = 0$  and acknowledging (3.10), (3.13) and (3.18), after integrating the equation (3.16) with respect to  $\xi$  we arrive at:

$$\frac{dp^1}{dz} = \text{const.} \Rightarrow p^1 = 0$$

due to  $p^1(0) = p^1(\frac{\ell}{R_1}) = 0$ . Finally, taking into account (3.11), from the equation (3.17) we obtain

$$(3.19) \quad T^1(\xi, z) = \frac{Br}{2\gamma Da^2} \left( \frac{\xi^4}{12} - \frac{\xi^5}{30} - \frac{\xi^3}{12} + \frac{\xi^2}{24} - \frac{\xi}{120} \right) \left( \frac{dp^0}{dz} \right)^2 + \frac{1}{2}(\xi - \xi^2),$$

due to  $T^1(0, z) = T^1(1, z) = 0$ . This completes the construction of the first-order correctors.

#### 4. Results and discussion

In view of the analysis presented in the previous section, the proposed approximations for the velocity and temperature take the following form:

$$(4.1) \quad \mathbf{u} = u\mathbf{e}_3 = (u_z^0 + \varepsilon u_z^1)\mathbf{e}_3, \quad T = T^0 + \varepsilon T^1.$$

The functions  $u_z^0$ ,  $T^0$ ,  $u_z^1$  and  $T^1$  appearing in the above asymptotic solution are given as follows (see (3.10), (3.11), (3.18) and (3.19)):

$$(4.2) \quad u_z^0 = \frac{C}{2Da} \xi(\xi - 1),$$

$$(4.3) \quad T^0 = \frac{BrC^2}{2\gamma Da^2} \left( \frac{\xi^3}{3} - \frac{\xi^4}{6} - \frac{\xi^2}{4} + \frac{\xi}{12} \right) + (1 - \xi),$$

$$(4.4) \quad u_z^1 = -\frac{C}{2\gamma Da} \left( \frac{\xi^3}{3} - \frac{\xi^2}{2} + \frac{\xi}{6} \right) \\ + \frac{RaBrC^2}{2\gamma^2 Da^3} \left( \frac{\xi^6}{180} - \frac{\xi^5}{60} + \frac{\xi^4}{48} - \frac{\xi^3}{72} + \frac{\xi}{240} \right) \\ - \frac{Ra}{\gamma Da} \left( \frac{\xi^3}{6} - \frac{\xi^2}{4} + \frac{\xi}{12} \right), \\ T^1 = \frac{BrC^2}{2\gamma Da^2} \left( \frac{\xi^4}{12} - \frac{\xi^5}{30} - \frac{\xi^3}{12} + \frac{\xi^2}{24} - \frac{\xi}{120} \right) + \frac{1}{2}(\xi - \xi^2),$$

for  $\xi \in \langle 0, 1 \rangle$  and  $\frac{dp^0}{dz} = C$ .

Having the solution in the explicit form, by looking at the characteristic numbers we can easily deduce the impact of the different flow parameters on the velocity and temperature distribution in the annular region. Namely, the effects of the porous structure are present in the approximation for the seepage velocity at the main order (see (4.2)). However, the zero-order approximation is not affected by the thermally-induced effects so we add the corrector (4.4) feeling the effects of the viscous dissipation. From (4.3), we conclude that the temperature distribution is affected by the viscous dissipation effects even at the main order. Comparing the results for the setting with neglected viscous dissipation where the heat flow is dominantly in the axial direction (see [25]), here we do not obtain such findings. It is also worth noticing that the convection term does not contribute to the temperature approximation and those effects would not appear even in the second-order corrector. Indeed, looking back to the (3.3), the equation satisfied by the corrector  $T^2$  reads:

$$1 : -\left(\frac{\partial^2 T^2}{\partial \xi^2} + \frac{\partial T^1}{\partial \xi}\right) = Br \left\{ \frac{1}{Da} \left(u_z^0\right)^2 + \gamma \left(\frac{\partial u_z^1}{\partial \xi}\right)^2 \right\}.$$

Applying the above expressions for  $u_z^0$ ,  $u_z^1$  and  $T^1$ , it is straightforward to explicitly compute  $T^2$  by taking into account that  $T^2(0, z) = T^2(1, z) = 0$  and we leave that to the interested reader. Although the contribution of the second-order term  $\varepsilon^2 T^2$  is negligible, observe that it captures the effects of the Darcy dissipation which are not present in the temperature approximation provided in (4.1).

Having in hand the explicit solution also enables us to visualize its behavior for different values of the characteristic numbers. Thus, in the following, using the application Graph, the numerical results are laid and discussed in detail. Namely, in Figures 2 and 3 we plot the velocity and temperature profiles provided in (4.1) for different values of the Brinkman number. By doing that, we clearly visualize the impact of viscous dissipation on the effective flow. Motivated by the practical examples of physical systems involving vertical annular flows in porous media where viscous dissipation effects are characterized by the higher Brinkman numbers, we choose  $Br \in \{100, 200, 300\}$ . The moderate value for the Rayleigh-Darcy number is  $Ra = 10^3$  (see e.g. [29]), while the Darcy number is taken as  $Da = 10^{-1}$ . We set the ratio  $\gamma = 1$ , whereas the axial pressure drop is given by  $C = -1$ . To ensure a thin-annular setting, we put  $\varepsilon = 10^{-3}$ .

Figure 2 clearly displays the behavior of the temperature profile with respect to the change of the Brinkman number. Due to the viscous dissipation, by gradually increasing the Brinkman number, the heat generation within the annular region raises, resulting in the significant increase in the fluid temperature. Also, it should be noticed that the fluid temperature exhibits rapid changes in the vicinity of the annular walls, while it becomes more flattened in between.

The viscous dissipation clearly raises the heat generation, resulting in the corresponding increase in the velocity of the working fluid as well. Indeed, by increasing the Brinkman number, a raise in the buoyancy force within the annular region occurs, so the effect of the viscous dissipation on the fluid velocity is more than obvious, as shown in Figure 3. It should be observed that the symmetry of the

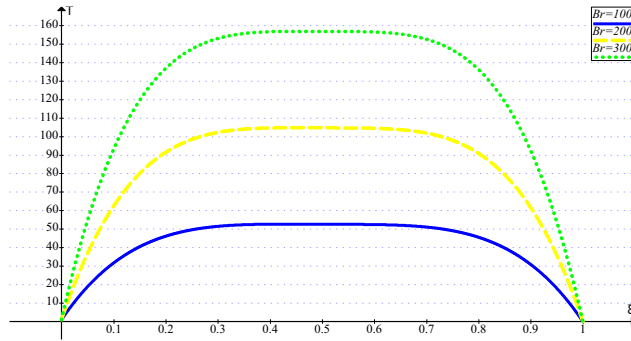


FIGURE 2. The effects of  $Br$  on the temperature profile (for  $\varepsilon = 10^{-3}$ ,  $Ra = 10^3$ ,  $Da = 10^{-1}$ ,  $\gamma = 1$  and  $C = -1$ ).

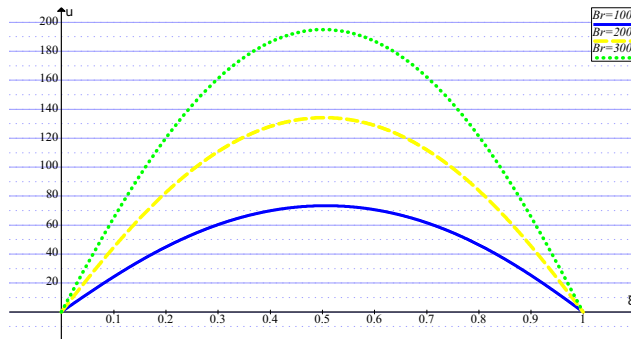


FIGURE 3. The effects of  $Br$  on the velocity profile (for  $\varepsilon = 10^{-3}$ ,  $Ra = 10^3$ ,  $Da = 10^{-1}$ ,  $\gamma = 1$  and  $C = -1$ ).

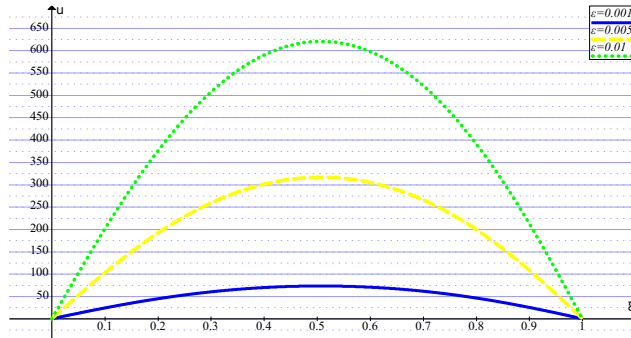


FIGURE 4. The effects of  $\varepsilon$  on the velocity profile (for  $Br = 100$ ,  $Ra = 10^3$ ,  $Da = 10^{-1}$ ,  $\gamma = 1$  and  $C = -1$ ).

velocity profile is mostly preserved since the viscous dissipation effects are carried by the corrector.

Last but not least, it is interesting to visualize how the thickness of the vertical annulus may influence the velocity of the working fluid. Figure 4 displays the velocity profile  $(4.1)_1$  for fixed  $Br = 100$  and varying thickness  $\varepsilon \in \{10^{-2}, 5 \cdot 10^{-2}, 10^{-3}\}$ . The other parameters are kept the same as in Figures 2 and 3. The results clearly suggest that the seepage velocity can be significantly increased by reducing the annulus thickness.

## 5. Conclusion

In this paper, an important application of the porous medium flow has been addressed: the non-isothermal flow through a thin annulus. We are particularly interested in viscous dissipation effects since this phenomenon became important in various geological processes and industrial applications. The framework with non-negligible viscous dissipation makes the standard Darcy-Brinkman-Boussinesq model (as considered in [25]) inappropriate, so we consider the generalization with additional term appearing in the energy equation, as proposed in [7]. After writing the problem in dimensionless form and passing to cylindrical coordinates, the asymptotic approximation of the flow is constructed using multi-scale expansion technique with respect to the annulus thickness. The main findings can be summarized as follows:

- The obtained asymptotic solution is given in the explicit form clearly showing the influence of the viscous dissipation.
- Increasing the Brinkman number leads to a significant raise of the velocity and temperature distribution within the annulus, due to the increase of the heat generation.
- Varying the thickness of the vertical annulus influences the velocity of the working fluid which can be used in the context of industrial applications design.

We believe that the provided results and numerical examples could prove useful in engineering practice. Chemical reactors with porous catalysts, geothermal energy extraction systems, and oil well casing annuli are only few physical systems involving vertical annular porous medium flow where viscous dissipation effects, characterized by Brinkman numbers  $Br \in \{100, 200, 300\}$ , are significant. Moreover, to the best of our knowledge, tackling this problem using analytical approach and without making substantial simplifications is still missing in the literature. The presented analysis can straightforwardly be extended to a case when an additional term of the form  $\mu_{eff} \mathbf{u}^* \cdot (\nabla^2 \mathbf{u}^*)$  is added in (1.4), as a result of power drag force related to the viscous dissipation (see [30]). Also, since the analytical solution has been derived in the explicit form, it can be employed as a control for numerical simulations. Our future work in this area will be devoted to theoretical error analysis of the given asymptotic model. This means that we aim to evaluate the difference between the original solution (that cannot be found) and the proposed asymptotic approximation in the suitable functional norm. To accomplish that,

we need to generalize the strategy from [22] to a fully coupled problem treated in the present paper. As a result, a rigorous justification of the proposed asymptotic approximation will be provided along with the information about its order of accuracy.

### Nomenclature

$\mathbf{u}^*$	velocity	$\mu$	physical viscosity
$\mathbf{u}^\varepsilon$	dimensionless velocity	$\mu_{eff}$	effective viscosity
$p^*$	pressure	$\gamma$	viscosity ratio
$p^\varepsilon$	dimensionless pressure	$\rho$	density
$T^*$	temperature	$C_f$	the specific heat
$T^\varepsilon$	dimensionless temperature	$\alpha$	thermal expansion
$\ell$	length of the cylinders	$T_r$	surrounding temperature
$R_1, R_2$	radii of the cylinders	$T_1, T_2$	prescribed temperatures
$\varepsilon$	small parameter	$g$	gravitational constant
$\Omega^*$	annulus	$U_0$	reference velocity
$k$	permeability	$Da$	Darcy number
$\lambda$	thermal conductivity	$Ra$	Rayleigh-Darcy number
$\Phi^*$	viscous dissipation term	$Br$	Brinkman number

**Acknowledgements.** The authors acknowledge the support of the Croatian Science Foundation under the project AsyAn (IP-2022-10-1091). The authors would like to thank the reviewer for his/her helpful comments and suggestions which helped to improve the paper.

### References

1. B. Gebhart, *Effects of viscous dissipation in natural convection*, J. Fluid Mech. **14** (1962), 225–232.
2. E. Magyari, D. A. S. Rees, B. Keller, *Effect of viscous dissipation on the flow in fluid saturated porous media*, In: K. Vafai (ed.), *Handbook of Porous Media*, 2<sup>nd</sup> ed., Taylor & Francis, New York, 2005, 373–406.
3. E. Sanchez-Palencia, *On the asymptotics of the fluid flow past an array of fixed obstacles*, Int. J. Eng. Sci. **20** (1982), 1291–1301.
4. G. Allaire, *Homogenization of the Navier–Stokes equations in open sets perforated with thin holes I. Abstract Framework, a volume distribution of holes*, Arch. Rational. Mech. Anal. **113** (1991), 209–259.
5. E. Marušić-Paloka, I. Pažanin, S. Marušić, *Comparison between Darcy and Brinkman laws in a fracture*, Appl. Math. Comput. **218** (2012), 7538–7545.
6. D. A. Nield, A. Bejan, *Convection in Porous Media*, 5<sup>th</sup> ed., Springer, New York, 2017.
7. A. K. Al-Hadhrami, L. Elliott, D. B. Ingham, *A new model for viscous dissipation in porous media across a range of permeability values*, Transp. Porous Med. **53** (2003), 117–122.
8. S. Husain, M. Adil, M. Arqam, B. Shaban, *A review on the thermal performance of natural convection in vertical annulus and its applications*, Renewable Sustain. Energy Rev. **150** (2011), 111463.
9. V. Prasad, F. A. Kulacki, A. V. Kulkarni, *Free convection in a vertical, porous annulus with constant heat flux on the inner wall—experimental results*, Int. J. Heat Mass Transf. **29** (1986), 713–723.
10. D. C. Reda, *Natural-convection experiments in a liquid-saturated porous medium bounded by vertical coaxial cylinders*, ASME J. Heat Transf. **105** (1986), 795.

11. B. M. R. Prasanna, M. Venkatachalappa, *Numerical study of natural convection in a vertical cylindrical annulus using a non-Darcy equation*, J. Porous Media **5**(2) (2002), 87–102.
12. M. Sankar, B. Jang, Y. Do, *Numerical study of non-Darcy natural convection from two discrete heat sources in a vertical annulus*, J. Porous Media **17** (2014), 373–390.
13. B. V. Pushpa, Y. Do, M. Sankar, *Control of buoyant flow and heat dissipation in a porous annular chamber using a thin baffle*, Indian. J. Phys. **96** (2022), 1767–1781.
14. K. Vajravelu, S. Sreenadh, G. Viswanatha Reddy, *Helical flow of a power-law fluid in a thin annulus with permeable walls*, Int. J. Non-Linear Mech. **41** (2006), 761–765.
15. K. Zhang, D. Kong, X. Liao, *On fluid flows in precessing narrow annular channels: Asymptotic analysis and numerical simulation*, J. Fluid Mech. **656** (2010), 116–146.
16. J.-S. Kuo, J. C. Leong, *Analysis of a conducting fluid in a thin annulus with rotating insulated walls under radial magnetic effect*, Appl. Math. Model. **37** (2013), 3021–3035.
17. A. V. Kuznetsov, *Analytical investigation of the fluid flow in the interface region between the porous medium and a clear fluid in channels partially filled with porous medium*, Flow Turbul. Combust. **56** (1996), 53–67.
18. A. Haji-Sheikh, D. A. Nield, K. Hooman, *Heat transfer in the thermal entrance region for flow through rectangular porous passages*, Int. J. Heat Mass Transf. **49** (2005), 3004–3015.
19. Y.-M. Hung, C. P. Tso, *Temperature variations of forced convection in porous media for heating and cooling processes: Internal heating effect of viscous dissipation*, Transp. Porous Med. **75** (2008), 319–332.
20. Y.-M. Hung, C. P. Tso, *Effects of viscous dissipation on fully developed forced convection in porous media*, Int. Commun. Heat Mass Transf. **36** (2009), 597–603.
21. B. K. Jha, J. O. Odengle, *Unsteady Couette flow in a composite channel partially filled with porous material: A semi-analytical approach*, Transp. Porous Media **107** (2015), 219–234.
22. I. Pažanin, M. Radulović, *Effects of viscous dissipation on the Darcy–Brinkman flow: Rigorous derivation of the higher-order asymptotic model*, Appl. Math. Comput. **386** (2020), 125479.
23. A. O. Ajibade, J. J. Gambo, B. K. Jha, *Effects of darcy and viscous Dissipation on natural convection flow in a vertical tube partiall filled with porous material under convective boundary condition*, Int. J. Appl. Comput. Math. **10** (2024), 84.
24. M. Beneš, I. Pažanin, *Rigorous derivation of the effective model describing a non-isothermal fluid flow through a vertical pipe filled with porous medium*, Contin. Mech. Thermodyn. **30** (2018), 301–317.
25. E. Marušić-Paloka, I. Pažanin, *On the thermal flow through a porous annular region*, J. Eng. Math. **147** (2024), 9.
26. H. I. Ene, D. Poliševski, *Thermal Flow in Porous Media*, Theory Appl. Transp. Porous Media, Springer, Dordrecht, 1987.
27. E. Marušić-Paloka, I. Pažanin, *Higher-order effective model describing a non-isothermal thin film flow*, Int. J. Multiscale Comput. Eng. **16**(2) (2018), 121–130.
28. I. Aganović, *An introduction to boundary value problems of continuum mechanics*, Element, Zagreb, 2003. (in Croatian)
29. S. Pirozzoli, M. De Paoli, M. Zonta, A. Soldati, *Towards the ultimate regime in Rayleigh–Darcy convection*, J. Fluid Mech. **911** (2021), R4.
30. D. A. Nield, *Comments on “A new model for viscous dissipation in porous media across a range of permeability values”*, by A. K. Al-Hadhrami, L. Elliott, D. B. Ingham, Transp. Porous Med. **55** (2004), 253–254.

## ЕФЕКТИ ВИСКОЗНЕ ДИСИПАЦИЈЕ КРЕТАЊА ФЛУИДА У ВЕРТИКАЛНОМ ПРСТЕНУ ИСПУЊЕНОГ ПОРОЗНОМ СРЕДИНОМ

**РЕЗИМЕ.** Истраживање преноса топлоте унутар порозне средине привукло је значајно интересовање због свог растућег практичног значаја. Овај рад је посвећен проучавању стационарног неизотермног струјања флуида кроз вертикални цилиндрични прстен испуњен ретко упакованом порозном средином. Систем једначина је дат Дарси-Бринкман-Бусинесковим моделом где једначина топлоте укључује члан вискозне дисипације. Бочни зидови се одржавају на једноликим температурама, док се ток покреће аксијалним градијентом притиска. Увођењем дебљине прстенасте области као малог параметра проблема, циљ је да се изведе апроксимација тока применом асимптотске анализе. Иако су једначине система спрегнуте и нелинеарне, предложено је асимптотско решење у експлицитном облику и то представља главни допринос рада. Као такво, јасно приказује ефекте порозне структуре и вискозне дисипације на расподелу температуре и брзине. Због вискозне дисипације, примећујемо повећање стварања топлоте што доводи до повећања температуре и профила брзине унутар прстена. Штавише, закључује се да смањење дебљине прстенасте области може бити примењено за повећање брзине цурења радног флуида. Такође, закључено је да се смањивањем дебљине прстена појачава брзина истицања флуида.

Department of Mathematics  
Faculty of Science  
University of Zagreb  
Croatia  
emarusic@math.hr  
<https://orcid.org/0000-0001-5770-8470>

(Received 11.03.2025)  
(Revised 16.05.2025)  
(Available online 05.06.2025)

Department of Mathematics  
Faculty of Science  
University of Zagreb  
Croatia  
pazanin@math.hr  
<https://orcid.org/0000-0003-3384-5184>